

pubs.acs.org/JACS Article

# Synthesis of Polycyclic Olefinic Monomers from Norbornadiene for Inverse Vulcanization: Structural and Mechanistic Consequences

Christopher M. Marshall, Jake Molineux, Kyung-Seok Kang, Vlad Kumirov, Kyung-Jo Kim, Robert A. Norwood, Jon T. Njardarson,\* and Jeffrey Pyun\*



Cite This: https://doi.org/10.1021/jacs.4c08113



**ACCESS** I

III Metrics & More

Article Recommendations

Supporting Information

**ABSTRACT:** The preparation of high-sulfur content organosulfur polymers has generated considerable interest as an emerging area in polymer science that has been driven by advances in the inverse vulcanization polymerization of elemental sulfur with organic comonomers. While numerous new inverse vulcanized polysulfides have been made over the past decade, insights into the mechanism of inverse vulcanization and structural characterization of the high-sulfur-content copolymers remain limited in scope. Furthermore, the exploration of new molecular architectures for organic comonomer synthesis



remains an important frontier to enhance the properties of these new polymeric materials. In the current report, the first detailed study on the synthesis and inverse vulcanization of polycyclic rigid comonomers derived from norbornadiene was conducted, affording a quantitative assessment of polymer microstructure for these organopolysulfides and insights into the inverse vulcanization polymerization mechanism for this class of monomers. In particular, a stereoselective synthesis of the endo-exo norbornadiene cyclopentadiene adduct (Stillene) was achieved, which enabled direct comparison with the known exo-exo norbornadiene dimer (NBD2) previously used for inverse vulcanization. Reductive degradation of these sulfur copolymers and detailed structural analysis of the recovered sulfurated organic fragments revealed that remarkable exo-stereospecificity was achieved in the inverse vulcanization of elemental sulfur with both these polycyclic dienyl comonomers, which correlated to the robust thermomechanical properties associated with organopolysulfides made from NBD2 previously. Melt processing and molding of these sulfur copolymers were conducted to fabricate free-standing plastic lenses for long-wave infrared thermal imaging.

# INTRODUCTION

Polymerizations with elemental sulfur have recently emerged as a field in polymer chemistry and sustainability as a route to high-sulfur content organopolysulfides which exhibit a wide range of intriguing (electro)chemical, optical, thermomechanical, rheological, and flame retardant properties. 1-6 The invention of the inverse vulcanization process by Pyun et al. in 2013 by the copolymerization of elemental sulfur  $(S_8)$  with 1,3-diisopropenylbenzene (DIB) has been a major driver of these advances via the melt copolymerization of S<sub>8</sub> with unsaturated monomers. In the past decade, the primary approach to enhancing the properties of high-sulfur content organopolysulfides made via inverse vulcanization (these polysulfides have been referred to as chalcogenide hybrid polymers (CHIPs) or inverse vulcanized polymers) has been through copolymerization of S<sub>8</sub> with conventional vinylic or olefinic comonomers, the significant scope of which can be read elsewhere. 1-6,8 Efforts to expand the scope of monomers for inverse vulcanization include improvements based on nucleophilic accelerators, 9,10 catalysts, 11,12 soluble sulfur prepolymers by dynamic covalent polymerizations 13-15 and photoinduced 16,17 polymerization methods. Novel anionic ring-opening copolymerization methods with  $S_8$  as pioneered by Penczek,  $^{18}$  have also been revisited with comonomer

variations, including Michael addition copolymerizations with acrylates and aziridines. 19-21 The groups of Lim, Hasell, and Chalker recently expanded inverse vulcanization processes to both episulfides (thiiranes) and epoxide comonomers.<sup>22-24</sup> The synthesis of novel olefinic monomers for inverse vulcanization has also been investigated in a much narrower scope for the incorporation of vinylic moieties to core skeletal architectures of interest, namely 1,3,5-triisopropenylbenzene,<sup>25</sup> thiophenes, <sup>26</sup> allyl terminated poly(3-hexylthiophene)<sup>27</sup> and notably most recently, perdeutero  $d_{14}$ -1,3-diisopropenylbenzene.<sup>28</sup> Alternatively, the use of other elemental sulfur-derived commodity chemicals such as sulfenyl chlorides (e.g.,  $S_2Cl_2$ ), and dithiophosphoric acids, have been used as monomers, or reagents for polymer synthesis. The synthesis and ring-opening polymerization of well-defined cyclic trisulfides,<sup>33</sup> or dithioacetals<sup>34</sup> has also been developed to prepare novel organopolysulfides.

Received: June 16, 2024 Revised: August 3, 2024 Accepted: August 5, 2024



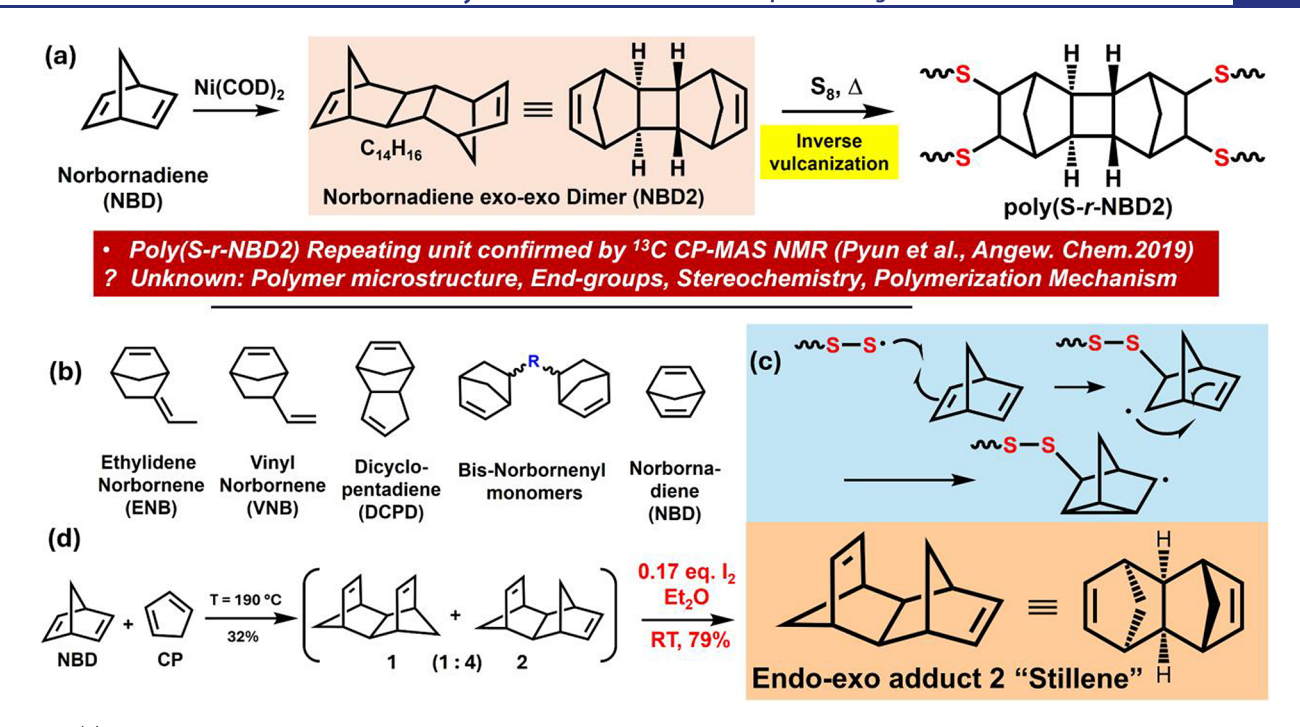


Figure 1. (a) Synthesis of NBD2 via dimerization of norbornadiene to afford the exo-exo dimer and inverse vulcanization with  $S_8$  to afford poly(S-r-NBD2). (b) Norbornene-based monomers reported for inverse vulcanization. (c) Side reactions encountered with radical reactions with norbornadiene. (d) Synthesis of "Stillene" (2), which is the endo-exo norbornadiene cyclopentadiene adduct, using a selective iodine-induced degradation approach to remove the undesired stereoisomer 1 by engaging its proximal olefins.

A notable advance to improve the optical and thermomechanical properties of high-sulfur content inverse vulcanized polysulfides was the Pyun group's synthesis and inverse vulcanization of the exo-exo dimer of norbornadiene (termed, NBD2), affording, poly(sulfur-random-norbornadiene dimer) (poly(S-r-NBD2), which exhibited one of the highest glass transition (Tg) values and highest degradation temperature onsets observed for sulfur polymers made by inverse vulcanization (Figure 1a). 35,36 Norbornene based monomers have been elegantly demonstrated by Hasell and co-workers<sup>11,37</sup> (e.g., ethylidene norbornene, vinyl norbornene, Figure 1b) to undergo inverse vulcanization, along with the use of dicyclopentadiene (DCPD) by Chalker and co-workers,<sup>38</sup> to tune thermomechanical properties. Further structural and mechanistic studies on the inverse vulcanization of DCPD, in conjunction with the application of the resulting polymers as coatings, were also investigated.<sup>39</sup> The inverse vulcanization of nonstrained cyclic olefins was demonstrated by Alhassan and co-workers, 40 along with a low-temperature mechanochemical reaction with norbornadiene<sup>41</sup> and inverse vulcanization with cyclopentadiene derived from DCPD.42 The coupling of monofunctional substituted norbornenes via (thio)ether linkers has been conducted to prepare bis-norbornenyl monomers which were subsequently applied to inverse vulcanization. However, the racemic mixture of endo- and exo-substituted norbornenes linked with flexible spacers only afforded low  $T_{\sigma}$ polymeric fluids.<sup>43</sup> Free radical polymerizations (and other chain reactions) using norbornadiene suffer from side reactions of carbon-centered radicals formed after the initial olefin addition with the neighboring olefin resulting in cycloaddition reaction intermediates to the norbornane skeleton (Figure 1c).44 Despite the successful inverse vulcanization of these norbornene and cyclic olefinic monomers, the tendency of norbornenes (e.g., ENB, VNB) to carbonize during inverse

vulcanization precludes the application of these materials as plastic optics (e.g., lenses, windows, fibers) for visible, or infrared applications despite possessing high glass transition values.<sup>6</sup> Furthermore, inverse vulcanized polysulfides derived from many aliphatic cyclic olefins possess low  $T_g$  values<sup>40</sup> precluding use as solid-state optical components. Conversely, the fused rigid symmetrical structure of NBD2 monomers suppresses intramolecular side reactions during radical reactions, 44 while also affording desirable thermomechanical properties, along with enhanced long wave infrared transparency (LWIR %T) and melt processability.<sup>35</sup> These advantages of poly(S-r-NBD2) were recently demonstrated in the first fabrication of LWIR plastic lenses which were successfully used for achieving room-temperature LWIR thermal imaging with sulfur-based plastics for the first time.<sup>45</sup> The highly cross-linked nature of poly(S-r-NBD2) was recently confirmed by small amplitude oscillatory rheology, where the presence of dynamic S-S bonds in these polymer networks rendered these dissociative covalent adaptive networks- $(CANs)^{36}$ 

The success of NBD2 and poly(S-r-NBD2) for inverse vulcanization and polysulfides with desirable properties warrants further investigation into the synthesis of related strained cyclic olefins to afford high-sulfur polymeric materials with desirable thermomechanical and optical properties. Furthermore, despite the recent work done to interrogate the bulk rheological and optical properties of poly(S-r-NBD2), mechanistic and structural studies of the final polysulfides have not yet been conducted, which is a critical step to enable definitive structure—property studies in the design of the next generation of polysulfide materials. To date, the only structural confirmation of the repeating unit of poly(S-r-NBD2) was conducted by Parker and Pyun and co-workers, 35 using 13C cross-polarization magic angle spinning NMR spectroscopy in

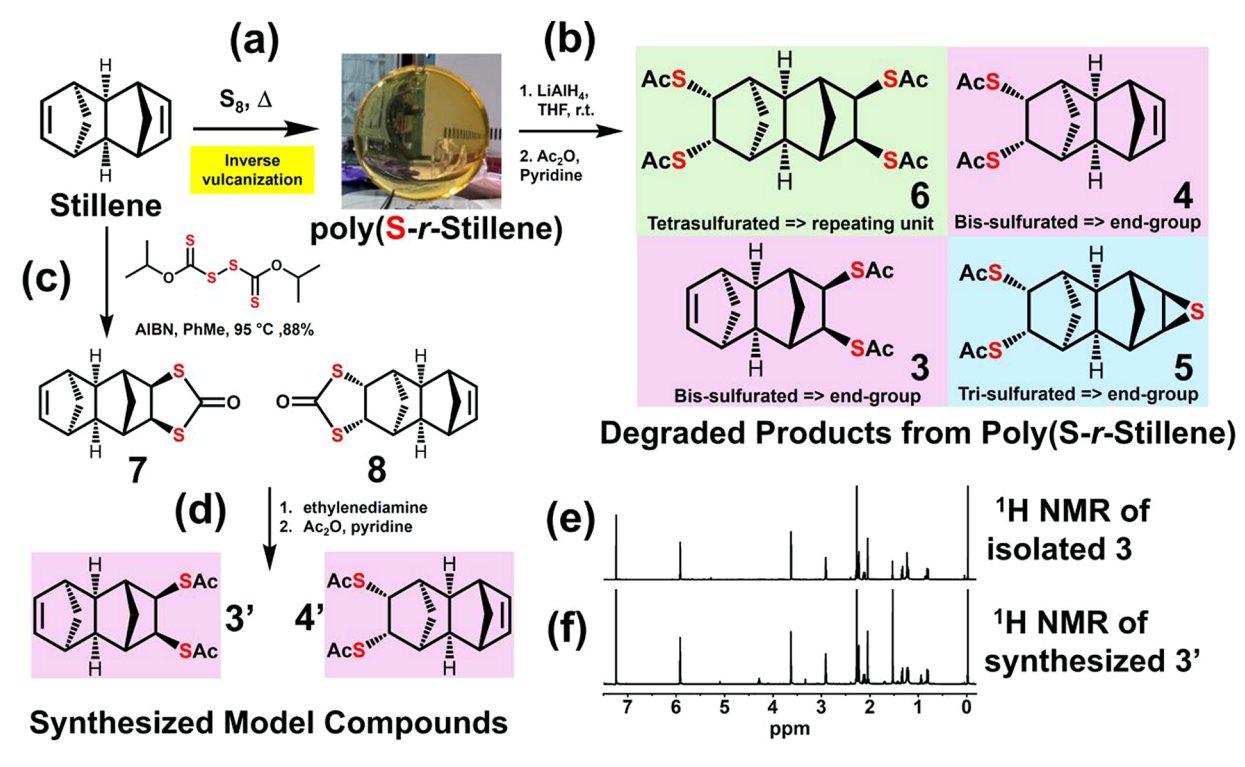


Figure 2. (a) Inverse vulcanization of Stillene to afford poly(S-r-Stillene) at both 50–70-wt % sulfur, 1 mm thick window of this polymer (50-wt % sulfur) shown (b) Reductive degradation of all S–S bonds of poly(S-r-Stillene) followed by acylation to afford degradation products 3, 4, 5 and 6, showing C–S bonds are all in exo-positions. (c and d) Synthesis of model compounds 3' and 4' exo- and endo-bis-dithioacetates from free radical reaction of Stillene with diisopropyl xanthogen disulfide (e) <sup>1</sup>H NMR spectrum of degraded product 3 from poly(S-r-Stillene) reduction vs (f) <sup>1</sup>H NMR spectrum of synthesized model compound 3' from Figure 2c,d vs recovered degradation product 3 from Figure 2a,b, confirming correct identification of degraded poly(S-r-Stillene).

the solid state (see Figure 1a summary), which precludes information on the exo-endo stereochemistry of C-S norbornyl bonds in poly(S-r-NBD2), possible end-groups, or minor alternative polymer microstructures. The chemical complexity of these types of studies is an issue in inverse vulcanized polysulfides due to the intractability of these materials at high-sulfur content compositions, along with the possibility for undesirable hydrogen atom abstraction side reactions to thiyl radical species in liquid sulfur. Hence, there remain limited mechanistic studies on the inverse vulcanization process despite the significant growth in activity in this new field. Notable exceptions include the recent report by Njardarson and co-workers<sup>46</sup> on the polymerization mechanism and structural studies on the inverse vulcanization of S<sub>8</sub> with DIB which notably enabled correct determination of the polymer microstructure of poly(S-r-DIB) by the reduction degradation of S-S bonds and structural characterization of the organic thiylated products. Model studies on monofunctionalized styrenics sulfurated with S<sub>8</sub> were also elegantly studied by Kanbara and co-workers. 47 However, mechanistic studies and microstructure conformations for norbornenebased monomers in inverse vulcanization remain unexplored.

Herein, we report the first detailed synthetic and structural study of inverse vulcanized polysulfides prepared from polycyclic rigid diene monomers derived from NBD. A selective and scalable synthesis of the endo-exo NBD adduct with cyclopentadiene (CP) is reported as well as the first studies on inverse vulcanization polymerizations with S<sub>8</sub>. Designer degradation methods of these novel organopolysulfides vs poly(S-r-NBD2) were conducted for the first time to reveal the correct polymer repeating unit for these materials,

which provided significant insight into the polymerization mechanism for the inverse vulcanization of these monomers with  $S_8$ . These structural studies reveal a remarkable degree of stereochemical control in the polymerization affording exclusively exo-exo thiyl radical additions to norbornyl olefins, which correlated to the high  $T_{\rm g}$  values observed in these sulfur copolymers. Finally, the desirable optical properties and melt processability of these materials are highlighted by fabrication into LWIR plastic optics and a demonstration of LWIR thermal imaging with these new polymers.

### ■ RESULTS AND DISCUSSION

Stereoselective Synthesis of Polycyclic Dienes from Norbornadiene. To expand the scope of possible strained cyclic olefins beyond NBD2, the synthesis of a designer norbornadiene-based diene was explored. The synthesis of the endo-exo tetracyclic Diels-Alder adduct 2 from norbornadiene and cyclopentadiene (CP) was targeted (Figure 1d), which retained the desired tetracyclic diene motif of the exo-exo NBD2 monomer but with a smaller carbon skeleton (C<sub>12</sub>H<sub>14</sub> vs C<sub>14</sub>H<sub>16</sub> for NBD2, Figure 1a,d). This new design increased the potential for higher sulfur-to-carbon ratios in the final sulfur copolymer materials with the aim of improving the LWIR transparency of the resulting sulfur copolymers vs poly(S-r-NBD2) without compromising the rigidity and thermomechanical properties of these materials. The synthesis of tetracyclic dienes via the reaction of norbornadiene with cyclopentadiene was initially reported by Stille and Frey via Diels-Alder methods which afforded mixtures of endo-exolinked stereoisomers. 48 To date these Diels-Alder cycloadducts have primarily been studied as monoene or diene

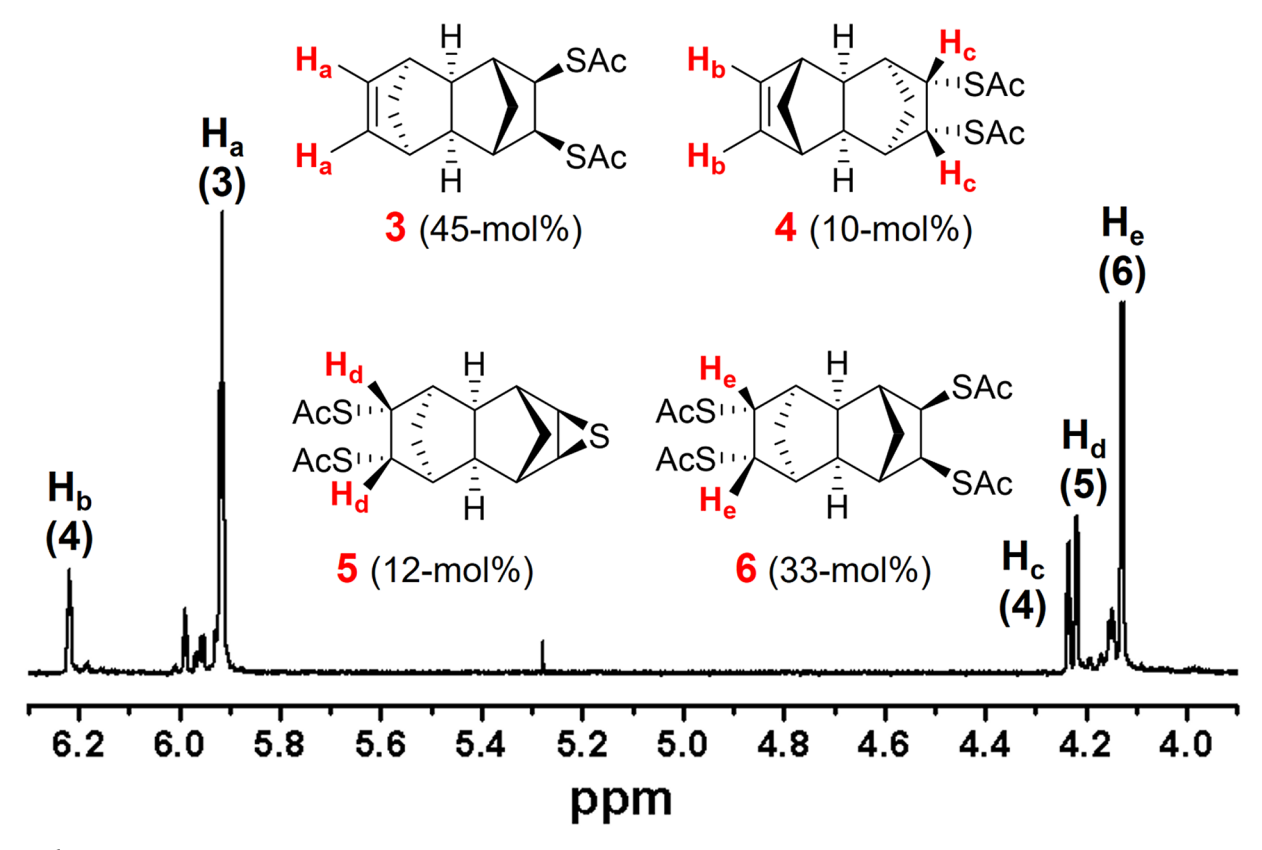


Figure 3.  $^{1}$ H NMR spectrum of crude acylated degradation product of poly(S-r-Stillene) containing 62-wt % sulfur after sequential reactions with LiAlH<sub>4</sub> and Ac<sub>2</sub>O, showing spectral peak assignments of recovered degradation products 3, 4, 5 and 6. From the molar ratios of this mixture, the exact microstructure of the original poly(S-r-Stillene) copolymer can be determined.

monomers for ring-opening metathesis polymerization (ROMP).<sup>49–51</sup> Related polycyclic dienes from NBD have been prepared, notably by the reaction of NBD with Ni(COD)<sub>2</sub> as demonstrated by Weinreb and co-workers,<sup>52</sup> which selectively affords the exo-exo NBD dimer (NBD2) along with trimers and oligomers, where sublimation of the NBD dimer is required to isolate the desired compound but consequently afforded high purity NBD2 material on a multigram scale. This exo-exo dimer of NBD, NBD2, is the only example of a strained polycyclic diene used for inverse vulcanization to date.<sup>35</sup> In related studies, Hawker and co-workers,<sup>53</sup> reported on the synthesis of functional norbornadiene-based compounds for a diverse array of polymer coupling reactions to prepare highly functionalized polymeric materials.

The improved total synthesis of 2 was initially conducted by Diels- Alder reaction of norbornadiene (NBD) with cyclopentadiene (CP) at elevated temperatures to afford stereoisomer cycloadducts 1 and 2 (Figure 1d), with isomer 2 representing the major product using the methods of Stille and Frey.<sup>48</sup> This stereoisomeric mixture could not be purified via chromatographic or distillation methods, which required Stille and co-workers to employ cumbersome and expensive silver nitrate complexation to separate 1 from 2. We realized that isomer 1, with its proximal olefins, would be detrimental to inverse vulcanization processes, as thiyl radical addition to these olefins would result in undesirable cyclization pathways that would suppress efficient polymerization. Hence, a more scalable and efficient synthetic strategy to separate isomer 1 from isomer 2 was achieved by employing transannular cyclizations via engagement with iodine  $(I_2)^{54,55}$  in various

solvents at room temperature. The proposed transannular cyclization reaction in diethyl ether of the undesired isomer (1) was observed to selectively proceed to enable facile isolation of desired endo-exo norbornadiene derived adduct 2 in good yields affording a colorless highly miscible liquid (79%, Figure 1d), which was herein referred to as the "Stillene"  $C_{12}H_{14}$  monomer to facilitate naming of the resulting sulfur copolymers after inverse vulcanization (as polycyclic multibridged alkane nomenclature is complex). To our knowledge, this methodology for the synthesis and isolation of stereoregular norbornadiene adducts has not been employed.

Synthesis and Structural Characterization of High-Sulfur Content Sulfur Copolymers via Inverse Vulcanization of Stillene. With Stillene in hand, the inverse vulcanization with S<sub>8</sub> was conducted with varying sulfur feed ratios (50-70 wt %) to prepare poly(sulfur-random-Stillene) (poly(S-r-Stillene). The neat Stillene liquid monomer was observed to be highly miscible in liquid sulfur (vs NBD2 which is a white crystalline solid) at elevated temperatures (T = 130°C) and rapidly polymerized within 5 min affording a transparent yellow glassy copolymer (Figure 2a). Higher temperature curing (T > 160 °C) afforded brown glassy polymeric materials. The bulk properties of poly(S-r-Stillene) were found to be comparable to the poly(S-r-NBD2) reference material with respect to refractive index as obtained from ellipsometry (n = 1.75 - 1.85) and thermal properties ( $T_{\sigma} > 100$ °C) for sulfur copolymers with 50-70 wt % sulfur (see Supporting Information, Figures S56, S51-55, respectively). This desirable combination of both high  $T_{\rm g}$  values and high refractive index for poly(S-r-Stillene) vs poly(S-r-NBD2) confirmed the benefits of these highly symmetrical rigid

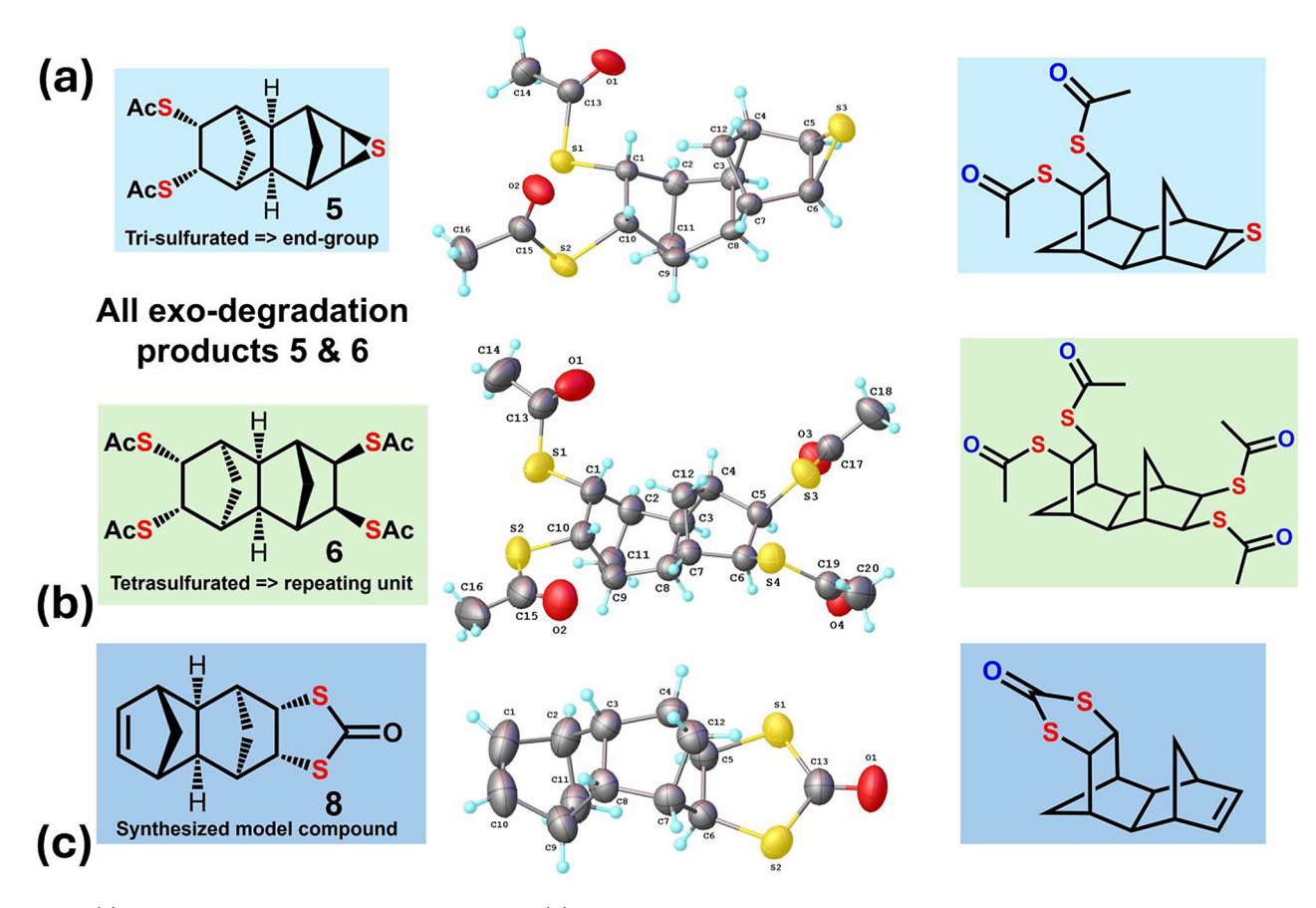


Figure 4. (a) Chemical structures and ORTEP view of 5, (b) Chemical structures and ORTEP view of 6, both from degradation and structural analysis of poly(S-r-Stillene) from Figure 2. (c) Chemical structures and ORTEP view of 8, both from degradation and structural analysis of poly(S-r-Stillene) from Figure 2.

tetracyclic motifs found in both polymers, which prompted detailed structural characterization of these materials. We previously conducted 13C CP-MAS NMR spectroscopy of poly(S-r-NBD2) (both 50 and 70 wt %), which confirmed the presence of terminal macro-olefinic groups and sulfuration of norbornenyl moieties which pointed to the tetrasulfurated NBD2 repeating unit proposed for poly(S-r-NBD2) (see Figure 1a).<sup>35</sup> However, more detailed structural analysis and mechanistic insights into the inverse vulcanization of S<sub>8</sub> and NBD2 have not yet been explored, particularly the stereochemical ratios of endo or exo isomers formed after thiyl radical addition to norbornenyl olefins. We recently reported on the first structural and computational mechanistic studies in the inverse vulcanization of S<sub>8</sub> with DIB, which revealed a different copolymer microstructure than initially proposed in the original 2013 publication, which pointed to the need for these types of detailed studies to enable accurate structureproperty materials correlations. 46 The poor solubility of highsulfur content polymers coupled with the potential for side reactions incurred in the reactive, high-temperature medium of liquid sulfur during inverse vulcanization has historically complicated these types of studies. Hence, to interrogate the correct microstructure of both poly(S-r-Stillene) and poly(S-r-NBD2), structural analysis was conducted after full reductive degradation of S-S bonds in the copolymer using lithium aluminum hydride (LiAlH<sub>4</sub>), followed by in situ acylation of thiols with acetic anhydride (Ac2O) in pyridine, which facilitated the recovery of stable sulfurated norbornenes, capped as thioesters, degradation products (Figure 2b).

The synthesis and degradation of poly(S-r-Stillene) was conducted for sulfur copolymers with 50, ~60, and 70 wt % sulfur to interrogate the microstructure of these materials versus varying sulfur monomer feed ratios from the inverse vulcanization polymerizations. These degradation and isolation efforts after silica gel chromatography revealed four sets of sulfurated organic molecules comprising the exo-syn-bisthioacetate/mono-olefin 3, along with its exo-anti-thioacetate/mono-olefin isomer 4, episulfide/dithioacetate 5, and tetra-thioacetate 6 as confirmed by 1D- and 2D <sup>1</sup>H and <sup>13</sup>C NMR spectroscopy (NMR spectroscopically determined molar ratios of 3:4:5:6 as shown in Figure 3). Recovered products 3, 4, 5 and 6 from the poly(S-r-Stillene) degradation were convincingly assigned by solution <sup>1</sup>H/<sup>13</sup>C NMR spectroscopy, mass-spectral analysis, and X-ray crystallography (in the case of episulfide 5 and tetrathioacetate 6, Figure 4a,b, see Supporting Information Figures S6-10 for 3; Figures S11-15 for 4; Figures S16-S20 for 5; and Figures S21-25 for 6). All of the degradation products from poly(S-r-Stillene) (3, 4, 5, and 6) were isolated by column chromatography allowing for the unambiguous assignment of <sup>1</sup>H and <sup>13</sup>C nuclei (along with high-resolution mass spectrometry confirmations). Hence, the determination of exact molar ratios of degradation compounds 3, 4, 5, and 6 was possible using the integration of wellresolved peaks from these molecules measured from <sup>1</sup>H NMR spectroscopy, as detailed below. Furthermore, unambiguous structural assignments of these degraded products were enabled by the synthesis of exact model compounds 3' and 4' by the norbornene addition of diisopropyl xanthogen

Table 1. Correlation of Sulfur Copolymer Composition on Poly(S-r-Stillene) Microstructures as a Function of Sulfur Content as Well as Results of Nickel-Catalyzed Stillene S<sub>8</sub>-Sulfuration

	Poly(S-r-Stillene) repeating unit from 6  Acs	Poly(S-r-Stillene) olefinic end group from 3	Poly(S-r-Stillene) olefinic end group from 4	Poly(S-r-Stillene) thiiriane end group from 5
Poly(S- <i>r</i> -Stillene) 50 wt% sulfur	25-mol%	52-mol%	13-mol%	10-mol%
Poly(S- <i>r</i> -Stillene) 62 wt% sulfur	33-mol%	45-mol%	10-mol%	12-mol%
Poly(S- <i>r</i> -Stillene) 70 wt% sulfur	64-mol%	22-mol%	11-mol%	3-mol%
Stillene-S <sub>8</sub> Ni-catalyst	40-mol%	20-mol%	12-mol%	28-mol%
	(a)	(b)	(c)	(d)

disulfide<sup>56</sup> to Stillene to form dithiocarbonates 7 and 8, which were separated and subjected to ethylenediamine and immediately acetylated with acetic anhydride to form 3' and 4', whose solution <sup>1</sup>H NMR spectra perfectly matched the samples obtained from degraded products 3 and 4 (Figure 2e,f). Furthermore, to comprehensively cover all possible sulfurated norbornene outcomes Stillene was also separately reacted with thioacetic acid to get the corresponding monoand bis-thioacetate Stillene adducts, which revealed no matches with any degradation products (3, 4, 5, and 6 from Figure 2) obtained from poly(S-r-Stillene) reduction and acylation. A <sup>1</sup>H NMR spectrum of the crude acylated degradation mixture of poly(S-r-Stillene) (product mixture from sulfur copolymer with 62 wt % sulfur shown in Figure 3) enabled unambiguous assignment of protons from comparison with <sup>1</sup>H NMR spectra of pure samples of each of the degradation products 3, 4, 5 and 6, where integration of these protons enabled determination of the original poly(S-r-Stillene) copolymer microstructure. The resolution in the <sup>1</sup>H NMR spectra of the discrete degradation products was striking and due to the chemical shift difference of olefinic, thiirane, and thioacetate moieties, which tremendously facilitated the integration of these <sup>1</sup>H NMR resonances to determine polymer microstructure molar compositions (Figure 3) as discussed in Table 1. Structural analysis of these isolated degradation products revealed that ALL of the C-S bonds from the acylated thiols on the Stillene C12 skeleton were exosubstituted, which pointed to stereospecific addition of thiyl radicals during the inverse vulcanization reaction to Stillene monomer olefinic groups. The presence of the thiirane moiety is a novel finding that aligns with the addition polymerization mechanism associated with the inverse vulcanization process, where the formation of exo-exo thiirane C-S bonds can be rationalized as a termination reaction of carbon-centered norbornyl radicals to S-S-S units via intramolecular addition-fragmentation processes. Evidence for this exospecific addition of thiyl radicals from S<sub>8</sub> to Stillene olefins was observed from the X-ray crystal structure of 5, which revealed that both thioacetate and thiirane groups were exosubstituted (Figure 4a). Furthermore, the X-ray crystal structure of tetrathioacetate degradation product 6 (Figure 4b) provided the most convincing evidence of all exo-specific addition of thiyl radicals from S<sub>8</sub> to Stillene during inverse vulcanization as this tetrasulfurated Stillene fragment was the key repeating unit formed in the sulfur copolymer. X-ray crystal structure of 8, (which was the dithiocarbonate precursor to model compound 4') was also collected, which confirmed the stereochemistry of the exo-exo addition to the less reactive olefin in Stillene (Table 1, mol-% composition of 3 vs 4) while importantly also unambiguously confirming the difference between structures 3 and 4 (Figure 4c). The crystal structure of 8 enabled a significant correlation of the synthetic route with the degradation route by firmly establishing the structure of 4' (synthetic derivative of 8), which in turn confirmed the structure of 3' (synthetic derivative of dithiocarbonate exo-isomer of 8, namely 7) and thus confirmations of synthetic 3' and 4' being the same structures as 3 and 4 obtained from designer S—S bond poly(S-r-Stillene) degradations. Additional definitive supportive structural evidence for the exo-specific addition during the inverse

Figure 5. Inverse vulcanization of NBD2 to afford poly(S-r-NBD2) at both containing both 50–70 wt % sulfur, 1 mm thick window of this polymer (50-wt % sulfur) shown followed by reductive degradation and acylation to afford degradation products 9, 10 and 11.

vulcanization of S<sub>8</sub> and Stillene was obtained via 2D NMR spectroscopy techniques (1H-1H COSY, HSQC and HMBC) as enabled by the numerous 4-bond (4J) "W-couplings" within the rigid Stillene framework of endo-protons on thioacylated carbons with bridgehead endo-protons and/or bridge methylene protons (see Supporting Information for full spectroscopy details for 3 (Figures S8-10), 4 (Figures S13-15), 5 (Figures S18-20), and 6 (Figures S23-25). The high fidelity of the degradation and structural analytical efforts described herein enabled precise structural insights into the microstructure and end-groups of poly(S-r-Stillene) made via inverse vulcanization (Table 1) along with sulfur copolymer composition effects on the polymer microstructure. The tetrasulfurated product 6 corresponded to the primary repeating unit of poly(S-r-Stillene) indicative of branch points in the highly cross-linked sulfur copolymer (Table 1a). Degraded, bis-sulfurated compounds 3 (Table 1b) and 4 (Table 1c) were assigned to terminal olefinic end-groups of the polymer but could also represent linear polymer units. Finally, the thiirane-bis-(sulfurate)-degradation product 5 (Table 1d) also was assigned to terminal end-groups from the poly(S-r-Stillene) copolymer. Analysis of the molar ratios of the polymer microstructures from 50 to 70 wt % sulfur in these poly(S-r-Stillene) materials demonstrate clear trends favoring a high content of the tetrasulfurated branched units derived from degradation product 6 (Table 1a), with higher monomer feed ratios of S<sub>8</sub> and higher sulfur content ranging from 25 to 64 mol %. This trend toward high sulfuration of organic Stillene units was anticipated for higher S<sub>8</sub> feed ratios in the inverse vulcanizations step. Interestingly, the reactivity of the nonequivalent norbornenyl double bonds in Stillene toward thiyl radical was manifested in the preferred formation of monoolefinic end-groups derived from degradation product 3 (Table 1b) vs the alternative mono-olefinic unit derived from degradation product 4 (~4:1 molar ratio) (Interestingly, this difference is marginal when xanthogen disulfide is utilized, Figure 2c). The preferred formation of thiirane terminal endgroups as derived from degradation product 5 (Table 1d) was observed to proceed when increasing sulfur composition and S<sub>8</sub> feed ratios from 50-wt % to 62-wt % sulfur, however, was

dramatically reduced at the higher 70-wt % sulfur composition and S<sub>8</sub> feed ratio due to the preferred tetrasulfuration pathway (Table 1a) Finally, the comparison of these poly(S-r-Stillene) microstructures determined with varying S<sub>8</sub> feed ratios in inverse vulcanization were compared with respect to stereochemistry and yield with sulfurated model compounds obtained by subjecting Stillene to nickel-catalyzed S<sub>8</sub> sulfurizations<sup>57</sup> (1 equiv Stillene, 1 equiv S<sub>8</sub>, 2 mol % [Ni(NH<sub>3</sub>)<sub>6</sub>]Cl<sub>2</sub> in DMF at 120 °C for 17 h) followed by reductive cleavage of the S-S bonds using LiAlH<sub>4</sub> and acetylation of the resulting free thiols with Ac<sub>2</sub>O in pyridine. These small molecule cyclic sulfides derived from Stillene exhibited similar overall trends for product distribution molar ratios, along with the exclusive stereochemical formation of exo C-S bonds, although a higher yield of thiirane-containing products was formed. These collective findings of all exo addition of in situ thiyl radicals to olefinic groups in Stillene during inverse vulcanization are consistent with the earlier literature on purely thermally driven reactions  $^{44}$  or nickel-catalyzed  $^{57,58}$  addition of  $S_8$  to norbornene.

Synthesis and Structural Characterization of High Sulfur Content Sulfur Copolymers via Inverse Vulcan**ization of NBD2.** The synthesis and degradation of poly(S-r-NBD2) was also conducted for sulfur copolymers with 50, ~60, and 70 wt % sulfur using the same degradation strategy as we had employed for poly(S-r-Stillene) to interrogate the microstructure of these materials versus varying sulfur copolymer composition. These methods afforded three sets of degradation products namely monoene/bis-sulfurated 9, monoepisulfide/bis-sulfurated 10 and tetrasulfurated 11 (Figure 5, see Supporting Information for full structural and 1D/2D NMR spectroscopic characterization for 9 (Figures S36-40), 10 (Figures S41-45), and 11 (Figures S46-50). The sulfurated degradation products of poly(S-r-NBD2) produced one less sulfurated fragment vs poly(S-r-Stillene) due to the higher symmetry of the exo-exo NBD2 skeleton vs the endo-exo-Stillene skeleton. Structural analysis of these isolated degradation products also revealed that ALL the C-S bonds from the acylated thiols on the NBD2 C<sub>14</sub> skeleton were exo-substituted, which pointed to stereospecific addition of

Table 2. Correlation of Sulfur Copolymer Composition on Poly(S-r-NBD2) Microstructures as a Function of the Sulfur Content

thiyl radicals during the inverse vulcanization reaction, just as described in the Stillene polymerization.

The degradation and structural analysis of poly(S-r-NBD2) also proceeded with high fidelity allowing for the determination of microstructures and end-groups formed by the inverse vulcanization of NBD2 (Table 2) along with sulfur copolymer composition effects on polymer microstructure. The tetrasulfurated product 11 corresponded to the primary repeating unit of poly(S-r-NBD2) indicative of branch points in the highly cross-linked sulfur copolymer (Table 2a), which was in agreement with the prior repeating structure determined from solid-state NMR spectroscopy.<sup>35</sup> Degraded, bis-sulfurated compound 9 (Table 2b) was assigned to terminal olefinic endgroups of the polymer, as will be discussed further below. Finally, the monoepisulfide/bis-sulfurated degradation product 10 (Table 2c) also was assigned to terminal end-groups from the poly(S-r-NBD2) copolymer. Analysis of the molar ratios of the polymer microstructures from 50 to 70 wt % sulfur in these poly(S-r-NBD2) materials revealed a more dramatic trend toward the formation of tetrasulfurated branched units derived from degradation product 11 (Table 2a) with higher monomer feed ratios of S<sub>8</sub> and higher sulfur content ranging from 32 to 85 mol %, which was a significantly higher molar fraction of these branched units than found in poly(S-r-Stillene) (Table 1). This trend toward high sulfuration of organic units was anticipated for higher S<sub>8</sub> feed ratios in the inverse vulcanizations step. The formation of monoene/bis-sulfurated endgroups derived from degradation product 9 was observed over the sulfur copolymer composition range from 50 to 70 wt %, consistent with similar units formed for poly(S-r-Stillene)

(Table 1b,c). However, the formation of monoepisulfide/bissulfurated unit derived from degradation product 11 was only observed to form at the lower sulfur copolymer composition (50 wt % sulfur) and was not recovered from poly(S-r-NBD2) materials possessing high-sulfur contents (62 wt %, 70 wt %). The higher content of tetrasulfurated branched units in poly(Sr-NBD2) in comparison to poly(S-r-Stillene) could possibly be attributed to its higher symmetry and the central cyclobutene ring, enhancing the reactivity of the double bonds in NBD2. Interestingly, when the sulfur content is increased in the inverse vulcanization reaction, the episulfide component disappears with a constant increase of tetrathioacetate 11, while bis-thioacetate 9 temporarily increases at the expense of episulfide 10 and then slowly gets consumed. It is also possible the elimination reactions with thiiranes are possible due to the thermally lability of these groups resulting in desulfurization with or without the presence of an activator.

Mechanistic Ramifications of These Structural Studies in the Inverse Vulcanization Process with Stillene and NBD2. Structural analysis of the degradation fragments isolated from the reduction of poly(S-r-Stillene) and poly(S-r-NBD2) enabled for the first time mechanistic insights into the inverse vulcanization mechanism of these architecturally similar monomers. With the structural information in hand, as previously discussed, we propose a polymerization mechanism for the stereospecific inverse vulcanization of Stillene and NBD2 that can be supported by the degradation/structural studies described in Figures 2 and 5. While numerous variations of these elementary reactions cannot be excluded, the proposed mechanism in Figure 6 focuses on the

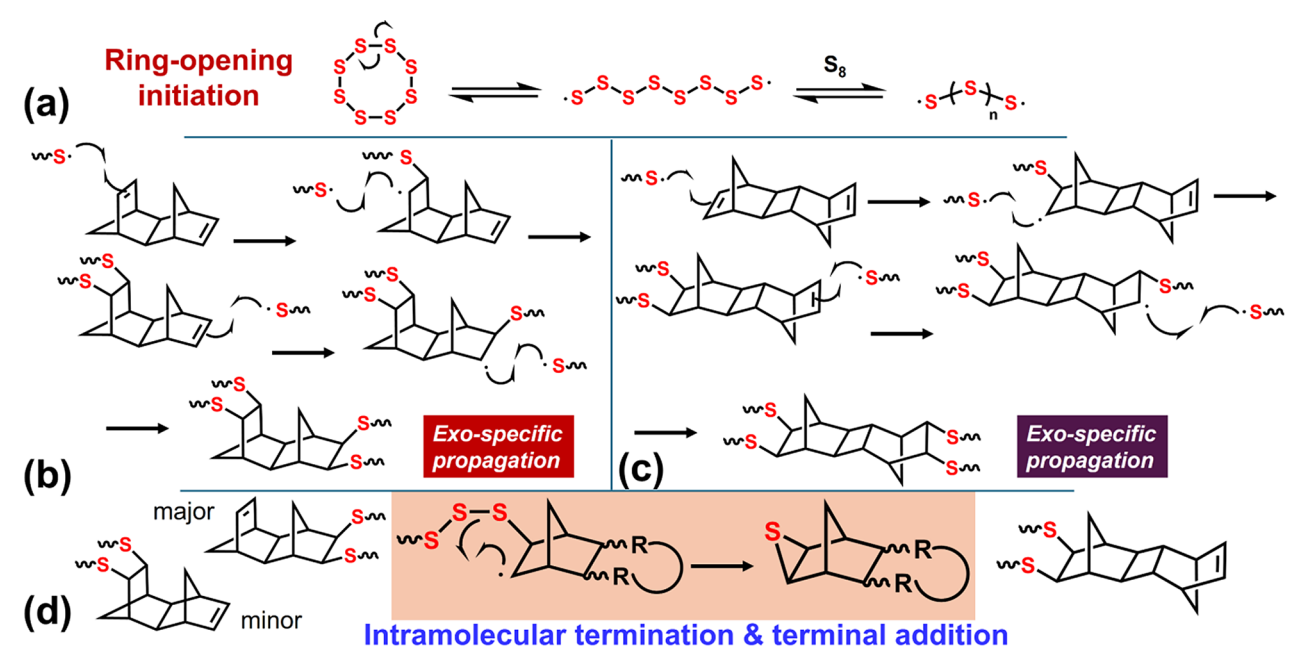
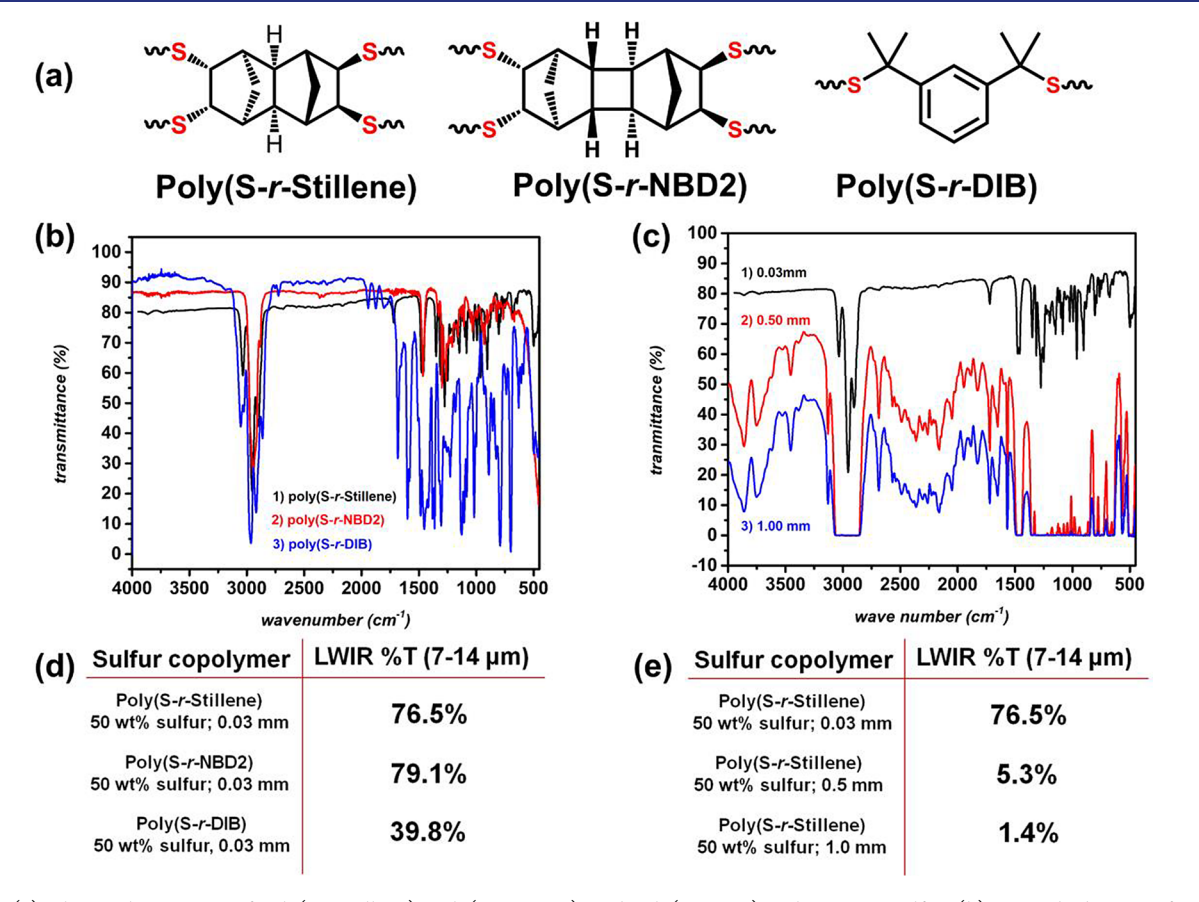


Figure 6. Proposed mechanism for the stereospecific inverse vulcanization of  $S_8$  with either Stillene or NBD2 proceeding via (a) ring-opening initiation of  $S_8$  (b) stereospecific exo-addition of thiyl radicals to olefinic groups of Stillene or (c) NBD2 (d) termination processes via intramolecular thiirane formation or terminal monoaddition to Stillene or NBD2.



**Figure 7.** (a) Chemical structures of poly(S-*r*-Stillene), poly(S-*r*-NBD2), and poly(S-*r*-DIB) with 50-wt % sulfur; (b) IR-stacked spectra for poly(S-*r*-Stillene, black), poly(S-*r*-NBD2, red), and poly(S-*r*-DIB, blue) thin films with thicknesses of 0.1 mm; (c) IR-stacked spectra for poly(S-*r*-Stillene) with windows of varying thicknesses from 0.1, 0.5, and 1.0 mm; (d) tabulation of LWIR %*T* samples in Figure 7b; and (e) tabulation of LWIR %*T* values for samples in Figure 7c.

1

most basic homolytic reactions likely to have occurred based on the structural studies previously described. It is also important to note that degradation and acylation chemistry used for these polymer microstructure studies can only inform

on the structure of the sulfurated organic comonomer units, which complicates the interpretation of mechanistic pathways involving dynamic S-S bond scission/reorganization. Initiation can be presumed to proceed via thiyl radical generation via homolysis of S<sub>8</sub> or other cyclic sulfur allotropes to form diradical linear species of varying chain lengths (Figure 6a). The exclusive isolation of exo-only substituted C-S fragments as summarized in Tables 1 and 2 points to a remarkable stereoselective propagation step of thiyl radical addition to norbornenyl groups of Stillene or NBD2 via a concerted, or stepwise fashion (stepwise mechanism shown in Figure 6b,c). This level of stereoselectivity is normally correlated to highly stereoregular polymers that possess semicrystalline morphologies as a consequence of improved chain packing in the solid state. However, due to the very high content of S-S bonds in the copolymer backbone, these effects are not observed, as evidenced by the DSC of only a single  $T_g$  for all of these sulfur copolymers. This type of stereospecificity has not been previously observed in any prior polymerizations with elemental sulfur, and, in conjunction with the stereoregular rigid architectures of NBD2 and Stillene, afford the unusually robust thermomechanical properties observed for both poly(Sr-NBD2) and poly(S-r-Stillene) at high sulfur copolymer content.<sup>36</sup> A related example was elegantly achieved by Chalker and co-workers, by the synthesis of an exo-exo norbornenyl cyclic trisulfide monomer and electrochemical polymerization of the single stereoisomer, where the exo-exo C-S bonds were preinstalled into the monomer and carried into the polymerization.<sup>33</sup> The isolation of episulfide fragments now enables the proposal of an intramolecular termination mechanism of carbon-centered radicals formed after the thiyl radical addition to the olefinic groups, which with lower sulfur feeds or higher S<sub>8</sub> conversions promote fragmentation of S-S bonds to form the exo-exo thiirane terminal end-group (Figure 6d, middle). The higher molar fractions of bis-sulfurated episulfide degradation products 5 and 10 (Figures 2 and 5) isolated at higher organic monomer feeds/reduced S<sub>8</sub> feeds corroborate this hypothesis. Furthermore, terminal monoaddition to Stillene affords two possible end-groups due to the inequivalent olefin reactivity in Stillene, along with a single possible terminal end group for the monoaddition of NBD2 (Figure 6d, left). We note that in the IR spectroscopic characterization of poly(S-r-Stillene) or poly(S-r-NBD2) high resolution of thicker films suggests some broad thiol S-H peaks are observed (2500-2000 cm<sup>-1</sup>, Figure 7c), however, these can be inferred to be the minor end-group products formed in these polymerizations. It is important to note that other polymerization pathways during the inverse vulcanization of these polycyclic dienes are possible, namely, the formation of cyclic sulfide terminal groups followed by thiyl radical ringopening, which would also preserve the all exo-stereochemistry of C-S bonds in the final organopolysulfides. However, due to the dynamic nature of S-S bond scission and reorganization, we present the most straightforward proposed polymerization mechanism in Figure 6 assuming only homolytic coupling processes.

IR Spectroscopic Characterization of Poly(S-r-Stillene) Windows and Comparison with State-of-the-Art Sulfur Copolymers. To demonstrate the potentially useful properties of poly(S-r-Stillene) materials, exploration of the refractive index, IR transmittance, and moldability into functional lenses were explored. High-sulfur content in organopolysulfides prepared via inverse vulcanization has

garnered significant interest as a new class of plastic optics for use in infrared (IR) thermal imaging, as the large fraction of S-S bonds are transparent in both the mid-wave (3-5  $\mu$ m;  $3000-2000 \text{ cm}^{-1}$ ) and long wave (7-14  $\mu$ m; 1200-700 cm<sup>-1</sup>) spectral regions that are most common for this application.<sup>8,32</sup> For these applications, highly dense, expensive inorganic materials (e.g., germanium, chalcogenide glass, and sapphire) are used as transmissive optical elements (e.g., lenses and windows) for IR imaging. Of particular interest for the broader consumer market application is the application of LWIR imaging systems in the 7-14  $\mu$ m region due to the relatively lower cost of LWIR vs MWIR detection systems. Thermal imaging in the LWIR spectrum is particularly challenging for hydrocarbon-based polymeric materials, as the vast majority of carbon-based covalent bonds (e.g., C-H, C-C, C-O, C-X) strongly vibrate and absorb this IR irradiation, which has been termed, the "Fingerprint region". 8,35 Inverse vulcanized polysulfides, also termed, Chalcogenide Hybrid Inorganic/Organic Polymers (CHIPs), 6,8 benefit from having a reduced fraction of organic comonomer units, however, the intense LWIR absorption of these organic moieties is still a major factor limiting the use of these materials for LWIR imaging. To date, several new sulfurbased comonomers have been explored to prepare candidate materials for LWIR imaging via inverse vulcanization, which include tetravinyltin, <sup>59</sup> dimeric norbornadiene (NBD2), <sup>35</sup> aryl halides, <sup>60</sup> benzene-1,3,5-trithiol, <sup>61</sup> 1,3,5-trivinylbenzene <sup>62</sup> norbornadiene, <sup>41</sup> and cyclopentadiene. <sup>42</sup> Poly(S-*r*-NBD2) is notable for possessing improved LWIR transparency and higher  $T_{\rm g}$  values versus existing inverse vulcanized polymers at high sulfur compositions. Due to the structural and compositional similarity of poly(S-r-Stillene) to poly(S-r-NBD2), IR characterization of this new polymer was conducted, along with fabrication via melt processing into free-standing LWIR

IR spectroscopy of thin 30  $\mu$ m films cast onto NaCl plates was initially conducted to comparatively access the MWIR and LWIR transmittance of poly(S-r-Stillene) vs the state-of-the-art LWIR inverse vulcanized polymer, poly(S-r-NBD2) and poly(S-r-DIB) (Figure 7b, all samples with 50-wt % sulfur composition). These measurements further enabled extrapolation to the LWIR transmittance of fabricated Fresnel lenses, as discussed shortly. To enable comparison of these transmittance values, the average transmittance (%T) values from 7 to 14 µm were obtained and determined directly from these IR spectroscopic measurements performed at room temperature. The stacked IR spectra for all of these sulfur copolymers confirmed optimal transmittance for poly(S-r-NBD2) (79.1-% T) and poly(S-r-Stillene) (76.5-%T) with significant reduction in LWIR transmission for the poly((S-r-DIB) (39.8-%T) thin films (Figure 7a,d). To enable the prediction of accessible acceptable thicknesses vs for targeted LWIR transmittance ranges for poly(S-r-Stillene) LWIR lenses, IR spectroscopic measurements for poly(S-r-Stillene) windows of increasing thickness of 0.03 0.5, and 1.0 mm were conducted, where the thicker windows were fabricated by molding the sulfur-Stillene melt resin into poly(dimethylsiloxane) (PDMS) molds and then polished to the target thickness (all possessing 50-wt % sulfur composition). The LWIR transmittance for these poly(S-r-Stillene) windows was observed to drop significantly with varying thickness from 76.5-%T (0.03 mm), 5.3% (0.5 mm), 1.4% (1.0 mm) (Figure 7c,e), which was consistent with similar thickness trends for poly(S-r-NBD2), with both

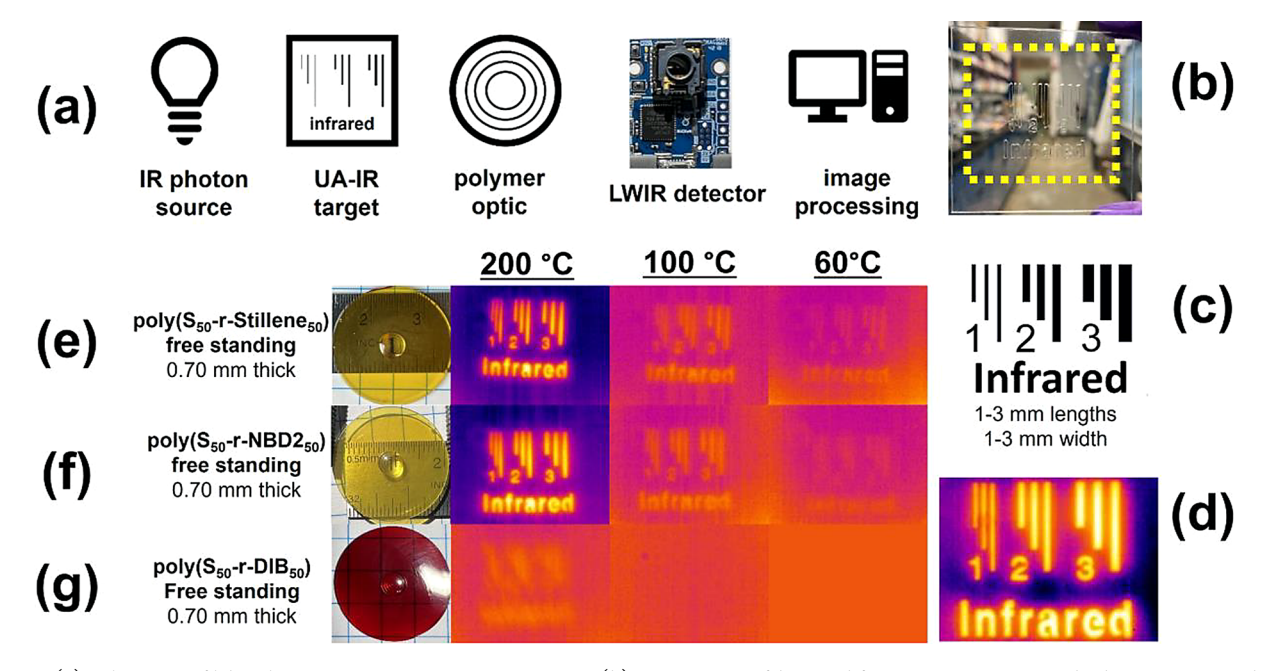


Figure 8. (a) Schematic of labscale prototype LWIR imaging system; (b) UA-IR target fabricated for LWIR imaging standardization prepared from  $CO_2$  laser writing into PMMA sheet; (c) specifications of UA-IR target pattern; (d) representative LWIR image of UA-IR target taken with a Ge lens reference; (e) LWIR imaging experiments conducted with the UA-IR target and labscale imaging system from Figure 8a from T = 200-60 °C for freestanding: (e) poly(S\_r-Stillene) Fresnel lens (0.7 mm thickness); (f) poly(S-r-NBD2) Fresnel lens (0.7 mm thickness); and (g) poly(S\_r-DIB) Fresnel lens (0.7 mm thickness).

significantly better than poly(S-r-DIB) (see Supporting Information).

Fabrication of LWIR Plastic Lenses and LWIR **Imaging.** An attractive feature of both poly(S-r-Stillene) and poly(S-r-NBD2) is the melt processing features of these materials to enable the molding of LWIR plastic lenses. We previously demonstrated the fabrication of LWIR flat diffractive optics using poly(S-r-NBD2) in the form of freestanding (0.7–1.0 mm) or thin film (0.1 mm) Fresnel lenses, along with integration into a lab scale LWIR imaging system (Figure 8a). 45 This basic benchtop LWIR imaging system was assembled using a hot plate/stirrer as the IR blackbody source in conjunction with a commercially available FLIR Lepton LWIR microbolometer detector. To enable standardization of LWIR imaging experiments, a custom-designed PMMA target fabricated by CO<sub>2</sub> laser was written into a PMMA sheet of hollow lines and numbers varying from 1 to 3 mm in length and width, and the word, Infrared, which when placed in front of a blackbody radiator, would create a well-defined optical resolution test chart, which was referred to as the University of Arizona Infrared Target (UA-IR target, Figure 8b,c). A model LWIR experiment done with a commercially available germanium (Ge) lens imaging the UA-IR target at room temperature was used as a reference for these experiments affording well-focused, high-resolution images of the UA-IR target features (Figure 8d). Using this LWIR imaging protocol, both free-standing and thin film poly(S-r-NBD2) were found to be capable of successful imaging, with improved resolution and focus being particularly evident in the thicker free-standing LWIR lenses vs poly(S-r-DIB). Using a similar melt casting protocol, poly(S-r-Stillene) with 50-wt % was fabricated into both free-standing and NaCl plate-supporting thin film Fresnel lenses (thickness = 0.7 mm, see Supporting Information for fabrication and characterization details). LWIR imaging results of the free-standing sulfur copolymer lenses (0.7 mm thick)

most profoundly illustrated the benefits of the improved LWIR transmittance of Fresnel lenses cast from both poly(S-r-Stillene) and poly(S-r-NBD2), where bright and clearly resolved imaging was still achieved at  $T=200~{}^{\circ}\mathrm{C}$  of the feature from the UA-IR target due to the higher IR photon flux at these higher temperatures, with imaging still achieved down to  $T=100~{}^{\circ}\mathrm{C}$ . LWIR imaging below  $T=60~{}^{\circ}\mathrm{C}$  with these same Fresnel lenses was not sufficiently bright or resolved due to the limited LWIR transmittance in this thickness range. Conversely, the control poly(S-r-DIB) free-standing Fresnel lens failed to achieve LWIR imaging even at the highest temperature  $T=200~{}^{\circ}\mathrm{C}$ , due to a combination of reduced LWIR transmittance and inferior thermomechanical properties.

# CONCLUSIONS

The synthesis, polymerization, and structural analysis of stereochemically pure norbornadiene-derived monomers for the inverse vulcanization process with elemental sulfur is reported, along with fabrication of these high-sulfur content materials into IR plastic optics for IR thermal imaging. A novel selective synthesis for the endo-exo norbornadiene cyclopentadiene Diels-Ader adduct (termed Stillene) was developed, along with successful copolymerization with elemental sulfur. The first structural analysis of inverse vulcanized polysulfides made from the endo-exo-Stillene and the exoexo NBD2 comonomers was conducted by reductive degradation and functionalization of free thiols degradation products to enable quantitative structural characterization of the microstructure of these sulfur copolymers. Using a combination of X-ray crystallography and NMR spectroscopic analysis of recovered degradation productions, evidence for a highly stereospecific process was observed for the inverse vulcanization with both Stillene and NBD2, which has previously not been observed. These findings provide

tremendous insight into the enhanced thermomechanical properties that arise from the inverse vulcanization of these rigid polycyclic monomeric motifs and further validate the importance of detailed mechanistic and structural studies for these polymerization processes to develop next-generation high-sulfur content polymeric materials.

#### EXPERIMENTAL METHODS

Synthesis of Endo-endo-Stillene (1) and Endo-exo-Stillene (2). Freshly distilled cyclopentadiene (8.00 g, 121 mmol, 1.0 equiv) and 2,5-norbornadiene (11.15 g, 121 mmol, 1.0 equiv) were added to a 35 mL glass pressure tube containing a PTFE-coated magnetic stir bar. The pressure tube was sealed with a PTFE bushing and immersed in a rapidly stirred preheated oil bath (T = 205 °C). The temperature of the oil bath was maintained at 200 °C over the course of the reaction. After heating for 13 h, the reaction vessel was removed from heating and cooled to room temperature. The crude reaction mixture was slightly yellow. An aliquot of the crude reaction mixture was removed for <sup>1</sup>H NMR analysis using CDCl<sub>3</sub> as the solvent. The collected <sup>1</sup>H NMR spectrum of the crude reaction mixture indicates the presence of endo-exo-Stillene (2) (42 mol %), endo-endo-Stillene (1, 10 mol %), unreacted NBD (48 mol %) and minor amounts of side products. The reaction mixture was transferred to a roundbottom flask using pentane. The mixture was concentrated by rotary evaporation. Then, the concentrated mixture was distilled under vacuum to afford a mixture of endo-exo-Stillene and endo-endo-Stillene (6.105 g, 38.6 mmol, 32% yield; 80.8 mol % endo-exo-Stillene, 19.2 mol %; endo-endo-Stillene; bp 46 °C, 0.24 Torr).

Isolation of Endo-exo-Stillene (2). A mixture of Stillene isomers (1.42 g, 8.97 mmol, 1.0 equiv) having a composition of endo-endo-Stillene (1) (16.9 mol %) and endo-exo-Stillene (2) (83.1 mol %) was added to a round-bottom flask containing a PTFE-coated stir bar, followed by diethyl ether (18 mL) and solid iodine (0.388 g, 1.53 mmol, 0.17 equiv). Upon adding iodine, the mixture turned dark red. The reaction mixture was stirred overnight at room temperature, at which point the green-brown mixture was quenched by adding aqueous 5% (w/v) Na<sub>2</sub>S<sub>2</sub>O<sub>3</sub> (20 mL). The resulting mixture was stirred vigorously and then transferred to a separatory funnel. The aqueous layer was separated, and the organic layer was washed with another portion of aqueous 5% (w/v) Na<sub>2</sub>S<sub>2</sub>O<sub>3</sub> (20 mL). The organic layer was separated, and the combined aqueous washes were extracted by using ethyl acetate (3 × 20 mL). The combined organic extracts were washed with brine (20 mL), dried over anhydrous Na<sub>2</sub>SO<sub>4</sub>, filtered, and concentrated in vacuo. A tan crystalline precipitate formed as the solvent was liberated. The concentrated mixture was purified by silica gel flash chromatography (eluted using hexanes) to afford pure endo-exo-Stillene (1.13 g, 7.14 mmol, 79% yield).

General Procedure Preparation of Poly(S-r-Stillene) with 50-wt % Sulfur. A 20 mL scintillation vial equipped with a PTFE-coated magnetic stir bar was charged with 1.00 g of elemental sulfur. The vial was placed in a preheated oil bath (155 °C) and stirred at 800 rpm until fully melted. Once completely liquid, 1.00 g of endo-exo-Stillene (2) was added via syringe to the vial, and the vial was capped. After 10 min, viscosity increased to the point at which the stir bar stopped stirring, and the reaction was cured for an additional 5 min. The reaction was then cooled to room temperature, and the material was recovered by freezing the vial in liquid nitrogen and fracturing the polymer from the vial. The final material was recovered as a glassy, yellow-orange material.

#### ASSOCIATED CONTENT

# **Supporting Information**

The Supporting Information is available free of charge at https://pubs.acs.org/doi/10.1021/jacs.4c08113.

Full experimental and characterization details (PDF)

#### **Accession Codes**

CCDC 2354405 and 2356341–2356342 contain the supplementary crystallographic data for this paper. These data can be obtained free of charge via www.ccdc.cam.ac.uk/data\_request/cif, or by emailing data\_request@ccdc.cam.ac.uk, or by contacting The Cambridge Crystallographic Data Centre, 12 Union Road, Cambridge CB2 1EZ, UK; fax: +44 1223 336033.

#### AUTHOR INFORMATION

#### **Corresponding Authors**

Jon T. Njardarson – Department of Chemistry and Biochemistry, University of Arizona, Tucson, Arizona 85721, United States; orcid.org/0000-0003-2268-1479; Email: njardars@arizona.edu

Jeffrey Pyun – Department of Chemistry and Biochemistry and C. Wyant College of Optical Sciences, University of Arizona, Tucson, Arizona 85721, United States;
Orcid.org/0000-0002-1288-8989; Email: jpyun@arizona.edu

#### **Authors**

Christopher M. Marshall – Department of Chemistry and Biochemistry, University of Arizona, Tucson, Arizona 85721, United States; orcid.org/0000-0001-5469-1378

Jake Molineux – Department of Chemistry and Biochemistry, University of Arizona, Tucson, Arizona 85721, United States

Kyung-Seok Kang — Department of Chemistry and Biochemistry, University of Arizona, Tucson, Arizona 85721, United States

Vlad Kumirov – Department of Chemistry and Biochemistry, University of Arizona, Tucson, Arizona 85721, United States Kyung-Jo Kim – C. Wyant College of Optical Sciences,

University of Arizona, Tucson, Arizona 85721, United States Robert A. Norwood — C. Wyant College of Optical Sciences, University of Arizona, Tucson, Arizona 85721, United States; Department of Materials Science & Engineering, College of Engineering, University of Arizona, Tucson, Arizona 85719, United States

Complete contact information is available at: https://pubs.acs.org/10.1021/jacs.4c08113

# **Author Contributions**

All authors have given approval to the final version of the manuscript.

#### **Notes**

The authors declare the following competing financial interest(s): Robert A. Norwood is an owner and officer of Norcon Technologies Holding, Inc with which a financial conflict of interest exists.

## ACKNOWLEDGMENTS

The National Science Foundation and the Air Force Research Laboratories are gratefully acknowledged for their support of this work through DMREF-2118578. We also acknowledge the Air Force Research Laboratories (FA8650-16-D-5404), the Hyundai Motor Company, and the University of Arizona, the Arizona Technology and Research Initiative Fund (A.R.S.§15-1648) for supporting this work. All NMR data were collected in the Nuclear Magnetic Resonance Facility, RRID:SCR\_012716, in the Department of Chemistry and Biochemistry at the University of Arizona. The purchase and upgrade of the Bruker AVANCE DRX 500 spectrometer was

partially supported by the National Science Foundation under Grant Numbers 9214383 and 9729350, the Office of Naval Research, and the University of Arizona. Dr. Andrei V. Astachkine and X-ray Diffraction (XRD) Facility, RRID:SCR\_022886, in the Department of Chemistry and Biochemistry of the University of Arizona, on a Philips PANalytical X'Pert PRO MPD instrument are gratefully acknowledged for support of X-ray crystallography.

### REFERENCES

- (1) Lim, J.; Pyun, J.; Char, K. Recent Approaches for the Direct Use of Elemental Sulfur in the Synthesis and Processing of Advanced Materials. *Angew. Chem., Int. Ed.* **2015**, *54*, 3249–3258.
- (2) Griebel, J. J.; Glass, R. S.; Char, K.; Pyun, J. Polymerizations with Elemental Sulfur: A Novel Route to High Sulfur Content Polymers for Sustainability. *Energy and Defense. Prog. Polym. Sci.* **2016**, *58*, 90–125.
- (3) Worthington, M. J. H.; Kucera, R. L.; Chalker, J. M. Green Chemistry and Polymers Made from Sulfur. *Green Chem.* **2017**, *19*, 2748–2761.
- (4) Chalker, J. M.; Worthington, M. J. H.; Lundquist, N. A.; Esdaile, L. J. Synthesis and Applications of Polymers Made by Inverse Vulcanization. *Top. Curr. Chem.* **2019**, *377*, 16.
- (5) Zhang, Y.; Glass, R. S.; Char, K.; Pyun, J. Recent Advances in the Polymerization of Elemental Sulphur, Inverse Vulcanization and Methods to Obtain Functional Chalcogenide Hybrid Inorganic/Organic Polymers (Chips). *Polym. Chem.* **2019**, *10*, 4078–4105.
- (6) Lee, T.; Dirlam, P. T.; Njardarson, J. T.; Glass, R. S.; Pyun, J. Polymerizations with Elemental Sulfur: From Petroleum Refining to Polymeric Materials. *J. Am. Chem. Soc.* **2022**, *144*, 5–22.
- (7) Chung, W. J.; et al. The Use of Elemental Sulfur as an Alternative Feedstock for Polymeric Materials. *Nat. Chem.* **2013**, *5*, 518–524.
- (8) Kleine, T. S.; Glass, R. S.; Lichtenberger, D. L.; Mackay, M. E.; Char, K.; Norwood, R. A.; Pyun, J. 100th Anniversary of Macromolecular Science Viewpoint: High Refractive Index Polymers from Elemental Sulfur for Infrared Thermal Imaging and Optics. *ACS Macro Lett.* 2020, *9*, 245–259.
- (9) Zhang, Y.; Kleine, T. S.; Carothers, K. J.; Phan, D. D.; Glass, R. S.; Mackay, M. E.; Char, K.; Pyun, J. Functionalized Chalcogenide Hybrid Inorganic/Organic Polymers (CHIPs) Via Inverse Vulcanization of Elemental Sulfur and Vinylanilines. *Polym. Chem.* **2018**, *9*, 2290–2294
- (10) Zhang, Y.; Pavlopoulos, N. G.; Kleine, T. S.; Karayilan, M.; Glass, R. S.; Char, K.; Pyun, J. Nucleophilic Activation of Elemental Sulfur for Inverse Vulcanization and Dynamic Covalent Polymerizations. *J. Polym. Sci. Part A. Polym. Chem.* **2019**, *57*, 7–12.
- (11) Wu, X.; Smith, J. A.; Petcher, S.; Zhang, B.; Parker, D. J.; Griffin, J. M.; Hasell, T. Catalytic Inverse Vulcanization. *Nat. Commun.* **2019**, *10*, 647.
- (12) Dodd, L. J.; Omar, Ö.; Wu, X.; Hasell, T. Investigating the Role and Scope of Catalysts in Inverse Vulcanization. *ACS Catal.* **2021**, *11*, 4441–4455.
- (13) Zhang, Y.; Konopka, K. M.; Glass, R. S.; Char, K.; Pyun, J. Chalcogenide Hybrid Inorganic/Organic Polymers (CHIPs) Via Inverse Vulcanization and Dynamic Covalent Polymerizations. *Polym. Chem.* **2017**, *8*, 5167–5173.
- (14) Karayilan, M.; Kleine, T. S.; Carothers, K. J.; Griebel, J. J.; Frederick, K. M.; Loy, D. A.; Glass, R. S.; Mackay, M. E.; Char, K.; Pyun, J. Chalcogenide Hybrid Inorganic/Organic Polymer Resins: Amine Functional Prepolymers from Elemental Sulfur. *J. Polym. Sci.* **2020**, *58*, 35–41.
- (15) Kang, K.; et al. Synthesis of Segmented Polyurethanes from Elemental Sulfur with Enhanced Thermomechanical Properties and Flame Retardancy. *Angew. Chem., Int. Ed.* **2021**, *60*, 22900–22907.
- (16) Jia, J.; et al. Photoinduced Inverse Vulcanization. *Nat. Chem.* **2022**, *14*, 1249–1257.

- (17) Ambulo, C. P.; Carothers, K. J.; Hollis, A. T.; Limburg, H. N.; Sun, L.; Thrasher, C. J.; McConney, M. E.; Godman, N. P. Photo-Crosslinkable Inorganic/Organic Sulfur Polymers. *Macromol. Rapid Commun.* **2023**, *44*, No. 2200798.
- (18) Penczek, S.; ŚLazak, R.; Duda, A. Anionic Copolymerisation of Elemental Sulphur. *Nature* **1978**, *273*, 738–739.
- (19) Gallizioli, C.; Battke, D.; Schlaad, H.; Deglmann, P.; Plajer, A. J. Ring-Opening Terpolymerisation of Elemental Sulfur Waste with Propylene Oxide and Carbon Disulfide Via Lithium Catalysis. *Angew. Chem., Int. Ed.* **2024**, *63*, No. e202319810.
- (20) Yang, H.; Huang, J.; Song, Y.; Yao, H.; Huang, W.; Xue, X.; Jiang, L.; Jiang, Q.; Jiang, B.; Zhang, G. Anionic Hybrid Copolymerization of Sulfur with Acrylate: Strategy for Synthesis of High-Performance Sulfur-Based Polymers. J. Am. Chem. Soc. 2023, 145, 14539—14547.
- (21) Huang, H.; Zheng, S.; Luo, J.; Gao, L.; Fang, Y.; Zhang, Z.; Dong, J.; Hadjichristidis, N. Step-Growth Polymerization of Aziridines with Elemental Sulfur: Easy Access to Linear Polysulfides and Their Use as Recyclable Adhesives. *Angew. Chem., Int. Ed.* **2024**, 63, No. e202318919.
- (22) Park, S.; Chung, M.; Lamprou, A.; Seidel, K.; Song, S.; Schade, C.; Lim, J.; Char, K. High Strength, Epoxy Cross-Linked High Sulfur Content Polymers from One-Step Reactive Compatibilization Inverse Vulcanization. *Chem. Sci.* **2022**, *13*, 566–572.
- (23) Yan, P.; Zhao, W.; Tonkin, S. J.; Chalker, J. M.; Schiller, T. L.; Hasell, T. Stretchable and Durable Inverse Vulcanized Polymers with Chemical and Thermal Recycling. *Chem. Mater.* **2022**, *34*, 1167–1178
- (24) Jeon, Y.; Choi, J.; Seo, D.; Jung, S. H.; Lim, J. Low Birefringence and Low Dispersion Aliphatic Thermosets with a High and Tunable Refractive Index. *Polym. Chem.* **2023**, *14*, 1117–1123
- (25) Kleine, T. S.; et al. High Refractive Index Copolymers with Improved Thermomechanical Properties Via the Inverse Vulcanization of Sulfur and 1,3,5-Triisopropenylbenzene. *ACS Macro Lett.* **2016**, *5*, 1152–1156.
- (26) Tavella, C.; Luciano, G.; Lova, P.; Patrini, M.; D'Arrigo, C.; Comoretto, D.; Stagnaro, P. 2,5-Diisopropenylthiophene by Suzuki–Miyaura Cross-Coupling Reaction and Its Exploitation in Inverse Vulcanization: A Case Study. *RSC Adv.* **2022**, *12*, 8924–8935.
- (27) Oschmann, B.; Park, J.; Kim, C.; Char, K.; Sung, Y.-E.; Zentel, R. Copolymerization of Polythiophene and Sulfur to Improve the Electrochemical Performance in Lithium–Sulfur Batteries. *Chem. Mater.* **2015**, 27, 7011–7017.
- (28) Qureshi, M. H.; et al. Synthesis of Deuterated and Sulfurated Polymers by Inverse Vulcanization: Engineering Infrared Transparency Via Deuteration. *J. Am. Chem. Soc.* **2023**, *145*, 27821–27829.
- (29) Kang, K.-S.; et al. Sulfenyl Chlorides: An Alternative Monomer Feedstock from Elemental Sulfur for Polymer Synthesis. *J. Am. Chem. Soc.* **2022**, *144*, 23044–23052.
- (30) Grace, J. P.; Flitz, E. S.; Hwang, D. S.; Bowden, N. B. Polymerization of Aniline Derivatives to Yield Poly[N,N-(Phenylamino)Disulfides] as Polymeric Auxochromes. *Macromolecules* **2021**, *54*, 10405–10414.
- (31) Olikagu, C.; Kumirov, V. K.; Njardarson, J. T.; Hahn, M. J.; Pyun, J. Nmr Spectroscopic Characterization of Polyhalodisulfides Via Sulfenyl Chloride Inverse Vulcanization with Sulfur Monochloride. *Polymer* **2024**, 290, No. 126539.
- (32) Bao, J.; Kang, K.; Molineux, J.; Bischoff, D. J.; Mackay, M. E.; Pyun, J.; Njardarson, J. T. Dithiophosphoric Acids for Polymer Functionalization. *Angew. Chem., Int. Ed.* **2024**, *63*, No. e202315963.
- (33) Pople, J. M. M.; Nicholls, T. P.; Pham, L. N.; Bloch, W. M.; Lisboa, L. S.; Perkins, M. V.; Gibson, C. T.; Coote, M. L.; Jia, Z.; Chalker, J. M. Electrochemical Synthesis of Poly(Trisulfides). *J. Am. Chem. Soc.* **2023**, *145*, 11798–11810.
- (34) Kariyawasam, L. S.; Highmoore, J. F.; Yang, Y. Chemically Recyclable Dithioacetal Polymers Via Reversible Entropy-Driven Ring-Opening Polymerization. *Angew. Chem., Int. Ed.* **2023**, *62*, No. e202303039.

- (35) Kleine, T. S.; et al. Infrared Fingerprint Engineering: A Molecular-Design Approach to Long-Wave Infrared Transparency with Polymeric Materials. *Angew. Chem., Int. Ed.* **2019**, *58*, 17656–17660.
- (36) Bischoff, D. J.; Lee, T.; Kang, K.-S.; Molineux, J.; O'Neil Parker, W.; Pyun, J.; Mackay, M. E. Unraveling the Rheology of Inverse Vulcanized Polymers. *Nat. Commun.* **2023**, *14*, 7553.
- (37) Smith, J. A.; Wu, X.; Berry, N. G.; Hasell, T. High Sulfur Content Polymers: The Effect of Crosslinker Structure on Inverse Vulcanization. *J. Polym. Sci. Part A. Polym. Chem.* **2018**, *56*, 1777–1781.
- (38) Smith, J. A.; et al. Crosslinker Copolymerization for Property Control in Inverse Vulcanization. *Chem.—Eur. J.* **2019**, 25, 10433–10440.
- (39) Mann, M.; Zhang, B.; Tonkin, S. J.; Gibson, C. T.; Jia, Z.; Hasell, T.; Chalker, J. M. Processes for Coating Surfaces with a Copolymer Made from Sulfur and Dicyclopentadiene. *Polym. Chem.* **2022**, *13*, 1320–1327.
- (40) Omeir, M. Y.; Wadi, V. S.; Alhassan, S. M. Inverse Vulcanized Sulfur—Cycloalkene Copolymers: Effect of Ring Size and Unsaturation on Thermal Properties. *Mater. Lett.* **2020**, 259, No. 126887.
- (41) He, L.; Yang, J.; Jiang, H.; Zhao, H.; Xia, H. Mechanochemistry Enabled Inverse Vulcanization of Norbornadiene for Optical Polymers and Elastomeric Materials. *Ind. Eng. Chem. Res.* **2023**, *62*, 9587–9594.
- (42) Tonkin, S. J.; Pham, L. N.; Gascooke, J. R.; Johnston, M. R.; Coote, M. L.; Gibson, C. T.; Chalker, J. M. Thermal Imaging and Clandestine Surveillance Using Low-Cost Polymers with Long-Wave Infrared Transparency. *Adv. Opt. Mater.* **2023**, *11*, No. 2300058.
- (43) Kwon, M.; Lee, H.; Lee, S.-H.; Jeon, H. B.; Oh, M.-C.; Pyun, J.; Paik, H.-J. Dynamic Covalent Polymerization of Chalcogenide Hybrid Inorganic/Organic Polymer Resins with Norbornenyl Comonomers. *Macromol. Res.* **2020**, *28*, 1003–1009.
- (44) Bartlett, P. D.; Ghosh, T. Sulfuration of the Norbornene Double Bond. J. Org. Chem. 1987, 52, 4937–4943.
- (45) Molineux, J.; Lee, T.; Kim, K. J.; Kang, K.-S.; Lyons, N. P.; Nishant, A.; Kleine, T. S.; Durfee, S. W.; Pyun, J.; Norwood, R. A. Fabrication of Plastic Optics from Chalcogenide Hybrid Inorganic/Organic Polymers for Infrared Thermal Imaging. *Adv. Opt. Mater.* **2024**, *12*, No. 2301971.
- (46) Bao, J.; Martin, K. P.; Cho, E.; Kang, K.-S.; Glass, R. S.; Coropceanu, V.; Bredas, J.-L.; Parker, W. O. N., Jr; Njardarson, J. T.; Pyun, J. On the Mechanism of the Inverse Vulcanization of Elemental Sulfur: Structural Characterization of Poly(Sulfur-Random-(1,3-Diisopropenylbenzene)). *J. Am. Chem. Soc.* **2023**, *145*, 12386–12397.
- (47) Onose, Y.; Ito, Y.; Kuwabara, J.; Kanbara, T. Tracking Side Reactions of the Inverse Vulcanization Process and Developing Monomer Selection Guidelines. *Polym. Chem.* **2022**, *13*, 5486–5493.
- (48) Stille, J. K.; Frey, D. A. Tetracyclic Dienes. I. The Diels-Alder Adduct of Norbornadiene and Cyclopentadiene. *J. Am. Chem. Soc.* 1959, 81, 4273–4275.
- (49) Alonso, M. A.; Farona, M. F. Homo- and Copolymerization of Some Norbornadiene Dimer Monomers. *Polym. Bull.* **1987**, *18*, 203–207.
- (50) Ding, R.; Xia, Y.; Mauldin, T. C.; Kessler, M. R. Biorenewable Romp-Based Thermosetting Copolymers from Functionalized Castor Oil Derivative with Various Cross-Linking Agents. *Polymer* **2014**, *55*, 5718–5726.
- (51) Hase, K.; Matsuoka, S.-I.; Suzuki, M. Four Stereoisomeric Norbornadiene Dimers Containing a Cyclopropane Ring: Romp, Polymer Properties, and Post-Polymerization Modification. *Macromolecules* **2022**, *55*, 6811–6819.
- (52) Feldman, K. S.; Bobo, J. S.; Ensel, S. M.; Lee, Y. B.; Weinreb, P. H. Template-Controlled Oligomerization Support Studies. Template Synthesis and Functionalization. *J. Org. Chem.* **1990**, *55*, 474–481.
- (53) St. Amant, A. H.; et al. Norbornadienes: Robust and Scalable Building Blocks for Cascade "Click" Coupling of High Molecular Weight Polymers. *J. Am. Chem. Soc.* **2019**, *141*, 13619–13624.

- (54) Uemura, S.; Fukuzawa, S.; Toshimitsu, A.; Okano, M.; Tezuka, H.; Sawada, S. Iodine-Induced Formation of Bicyclo[3.3.0]Octane Derivatives from 1,5-Cyclooctadiene. *J. Org. Chem.* **1983**, 48, 270–273.
- (55) Günbaş, D. D.; Algı, F.; Hökelek, T.; Watson, W. H.; Balci, M. Functionalization of Saturated Hydrocarbons. High Temperature Bromination of Octahydropentalene. Part 19. *Tetrahedron* **2005**, *61*, 11177–11183.
- (56) Gareau, Y.; Beauchemin, A. Free Radical Reaction of Disopropyl Xanthogen Disulfide with Unsaturated Systems. *Heterocycles* **1998**, 48, 2003–2017.
- (57) Poulain, S.; Julien, S.; Duñach, E. Conversion of Norbornene Derivatives into Vicinal-Dithioethers Via S8 Activation. *Tetrahedron Lett.* **2005**, 46, 7077–7079.
- (58) Chapovetsky, A.; Haiges, R.; Marinescu, S. C. Synthesis and Characterization of a Tetranickel Complex Supported by a Dithiolate Framework with Pendant Ether Moieties. *Polyhedron* **2017**, *123*, 9–13
- (59) Boyd, D. A.; Nguyen, V. Q.; McClain, C. C.; Kung, F. H.; Baker, C. C.; Myers, J. D.; Hunt, M. P.; Kim, W.; Sanghera, J. S. Optical Properties of a Sulfur-Rich Organically Modified Chalcogenide Polymer Synthesized Via Inverse Vulcanization and Containing an Organometallic Comonomer. ACS Macro Lett. 2019, 8, 113–116.
- (60) Lee, J. M.; Noh, G. Y.; Kim, B. G.; Yoo, Y.; Choi, W. J.; Kim, D.-G.; Yoon, H. G.; Kim, Y. S. Synthesis of Poly(Phenylene Polysulfide) Networks from Elemental Sulfur and P-Diiodobenzene for Stretchable, Healable, and Reprocessable Infrared Optical Applications. ACS Macro Lett. 2019, 8, 912–916.
- (61) Lee, M.; Oh, Y.; Yu, J.; Jang, S. G.; Yeo, H.; Park, J.-J.; You, N.-H. Long-Wave Infrared Transparent Sulfur Polymers Enabled by Symmetric Thiol Cross-Linker. *Nat. Commun.* **2023**, *14*, 2866.
- (62) Hwang, J. H.; Kim, S. H.; Cho, W.; Lee, W.; Park, S.; Kim, Y. S.; Lee, J.-C.; Lee, K. J.; Wie, J. J.; Kim, D.-G. A Microphase Separation Strategy for the Infrared Transparency-Thermomechanical Property Conundrum in Sulfur-Rich Copolymers. *Adv. Opt. Mater.* 2023, 11, No. 2202432.